PHYSICAL REVIEW E **72**, 035201(R) (2005)

Spatiotemporal chaos in excised larynx vibrations

Yu Zhang and Jack J. Jiang
Department of Surgery, Division of Otolaryngology Head and Neck Surgery, University of Wisconsin Medical School, Madison, Wisconsin 53792-7375

(Received 24 November 2004; published 22 September 2005)

Spatiotemporal chaos in excised larynx vibrations is reported using high-speed digital imaging. Spatiotemporal correlation and eigenmode analyses are applied to describe the spatiotemporal dynamics of the vocal fold vibrations and to investigate the effects of subglottal pressure. High subglottal pressures cause spatiotemporal chaos with decreased spatiotemporal correlation and increased entropy in the vocal fold vibrations. Spatiotemporal analysis shows a valuable biomedical application in investigating the spatiotemporal chaotic dynamics of the vocal fold system.

DOI: 10.1103/PhysRevE.72.035201 PACS number(s): 05.45.Tp, 43.70.+i

Spatially extended systems such as Taylor-Coquette flow [1], Rayleigh-Bernard convection [2], the atmosphere [3], lasers [4], coupled-map lattices [5,6], fibrillating hearts [7], cellular flames [8], and the mammalian visual cortex system [9] have extremely complicated spatiotemporal dynamics. The spatial-temporal chaos of spatially extended systems has recently become the subject of intensive experimental and theoretical investigations [1–10]. In this study, we report the spatiotemporal chaotic vibratory behavior in a biomedical vocal fold system. As well as modeling vocal tracts [11], studying vibratory dynamics of the vocal folds is important for natural voice productions. Disordered voices are associated with laryngeal pathologies such as laryngeal paralysis and vocal mass lesions. The study of temporal instability in disordered voices has received considerable interest in the field of voice science [12–16]. Temporal chaos has been observed in animal vocalizations and human voices using time series analysis and [12,13] and lumped-parameter models of the vocal folds [14–16]. However, neither these chaotic models nor chaotic time series analyses have revealed the spatial complexities of the vocal fold vibrations. Spatial variations of the vibratory dynamics of the vocal folds have only recently been investigated [17–19]. This paper, to our knowledge, is the first time that the spatiotemporal chaotic vibration of the vocal folds has been measured with high-speed digital imaging. Spatiotemporal correlation and eigenmode analyses are applied to describe the spatiotemporal chaotic dynamics of vocal fold vibrations and to investigate the effect of subglottal pressure.

Excised larynx experiments facilitate direct observation and measurement of vocal fold vibrations, and have proven to be advantageous in the study of laryngeal physiology [20–23]. The experimental system consisted of an excised larynx setup and a high-speed camera system [Fig. 1(a)]. A canine larynx harvested from a healthy laboratory dog was used in an experimental trial 12–36 h after excision. The freshly excised canine larynx was mounted with a section of trachea on top of a pipe, and the trachea was tightly clamped to the pipe. A 3-pronged device was used to stabilize the arytenoid cartilages bilaterally, allowing for micrometer control of the distance between the vocal folds. A second micrometer system was attached by stitching a rod to the anterior tip of the thyroid lamina. Turning this micrometer system controlled the vocal fold tension by elongating the vocal folds. During the experiments, vocal fold tension and distance were held constant since the micrometer systems were unchanged.

The airflow was generated using an Ingersoll-Rand (Type 30) conventional air compressor and measured as it passed through a Gilmont rotameter-type flowmeter (J197). The input air was conditioned to 35–38 °C and 95%–100% relative humidity with two ConchaTherm III heater-humidifiers (Respiratory Care, Inc.) placed in series. The subglottal pres-

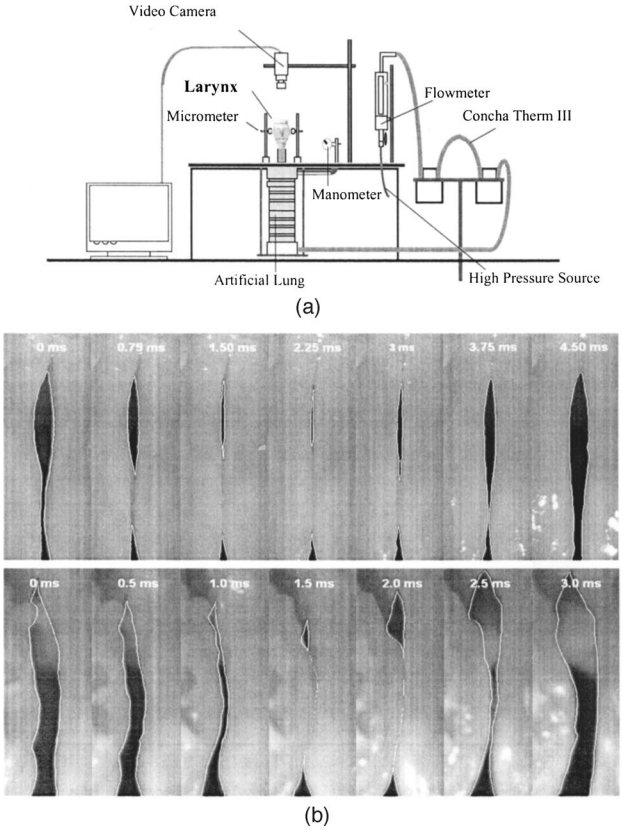

FIG. 1. (a) The experimental system consists of an excised larynx setup and a high-speed camera. (b) High-speed images of vocal fold vibration, where the upper and lower images correspond to subglottal pressure P_s=6 cm H_2O and 36 cm H_2O, respectively.

sure (P_s) in the artificial lung was measured with an open-ended water manometer (Dwyer No. 1211). When P_s was less than a threshold pressure [22], which was measured as 3 cm H_2O in this experiment, the larynx did not vibrate. When P_s was increased above 3 cm H_2O, the larynx began to vibrate.

A high-speed digital camera was mounted vertically above the larynx. The high-speed digital camera system acquired images at a sampling rate of 4000 frames per second with a resolution of 256×512 pixels. The image data was stored in digital form on a computer. The vocal fold edges were extracted using image edge detection on a frame-by-frame basis. Thresholding was used as the image edge detection method to separate the glottal area from the surrounding vocal fold tissue in an image by using 1's to indicate the glottal opening and 0's to indicate the surrounding vocal fold tissue. Figure 1(b) shows seven successive frames of the glottal edges at the subglottal pressure $P_s=6$ cm H_2O (the upper row) and $P_s=36$ cm H_2O (the lower row), respectively, where the white points mark the glottal edge. The glottis at the low pressure of 6 cm H_2O shows regular shapes, differing from the irregular shapes observed at the high pressure of 36 cm H_2O.

From the anterior side (thyroid cartilage) to the posterior side (arytenoid cartilage), the image of the glottis was divided into 108 horizontal segments with spatial index $j=1,2,\ N\ (N=108)$. Each segment shows the oscillation behavior $u(j,t)$ with respect to time. Thus, the spatiotemporal vibratory patterns of the vocal folds were recorded using high-speed digital imaging. Figures 2(a) and 2(b) show the spatiotemporal plots of $P_s=6$ and 36 cm H_2O, respectively. In comparison with the low subglottal pressure that produced regular spatiotemporal vibratory patterns and normal phonations, the high driving pressure produced irregular spatiotemporal vibratory patterns and rough sounds.

To study the spatiotemporal correlation of $u(j,t)$, we calculated the cross correlation function $C(i,j,\tau)$, which is defined as [24],

$$C(i,j,\tau)=\frac{\langle \delta u(i,t)\,\delta u(j,t+\tau)\rangle_T}{\sqrt{\langle \delta u(i,t)^2\rangle_T \langle \delta u(j,t)^2\rangle_T}}, \qquad (1)$$

where $\delta u(i,t)=u(i,t)-\langle u(i,t)\rangle_T$ and $\langle \bullet \rangle_T$ denotes the time average. For all the values of the delay time τ, the maximal value $C_{\max}(i,j)$ of $C(i,j,\tau)$ describes the spatial coherence of $u(j,t)$. We placed the spatial reference point with spatial index $j=54$ at the center of the glottis. As the spatial index i increases, a slowly decreasing $C_{\max}(i)$ indicates a spatiotemporally ordered pattern, while a rapidly decreasing $C_{\max}(i)$ is associated with spatiotemporal chaos. In order to quantitatively measure the spatiotemporal correlation, we define the following normalized correlation length as

$$L=(\,i_1|_{C_{\max}(i_1)=0.9}-\,i_2|_{C_{\max}(i_2)=0.9})/L_g \times 100\,\%\,, \qquad (2)$$

where L_g denotes the glottal length, i_1 and i_2 represent the two spatial points at which $C_{\max}(i_1)$ and $C_{\max}(i_2)$ decrease to 0.9 with respect to the reference point $j=54$. Correlation length L measures the size of the spatially ordered structure. A higher value of L corresponds to a larger size of the spatially ordered pattern. Data with complete spatial consistency has $L=100\%$; however, the correlation length of random spatiotemporal data approaches zero since any two spatial points are uncorrelated.

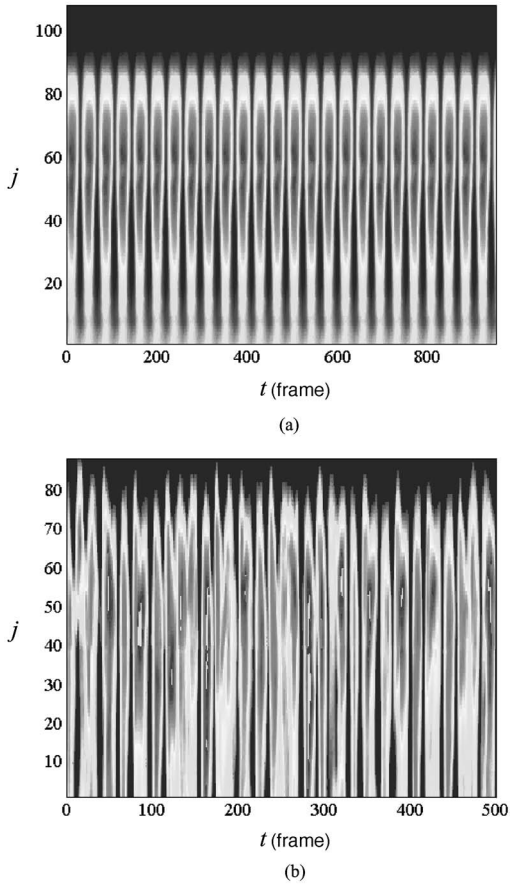

FIG. 2. The spatiotemporal plots of $u(j,t)$ at two subglottal pressure values. (a) $P_s=6$ cm H_2O. (b) $P_s=36$ cm H_2O.

Figure 3(a) shows the curves of $C_{\max}(i)$ vs i, where the curves from top to bottom correspond to $P_s=6$, 16, 26, and 36 cm H_2O. The spatial correlation lengths L of these four driving pressures are given in Table I, where a sine series with uniform spatial distribution and a random spatiotemporal series are also given for comparison. For these two cases, the spatial correlation lengths L are calculated as 100% and 0%, respectively. For $P_s=6$ cm H_2O, a high spatial correlation function $C_{\max}(i)$ shows high spatial symmetry of the glottis from the anterior to posterior sides. The spatial correlation length (96.8%) sufficiently approaches 100% indicating a highly ordered spatiotemporal state. However, the increase of P_s to 16 and 26 cm H_2O decreases the spatial coherence and correlation length, and increases the degree of asymmetry of the vocal fold vibrations. Anterior-posterior asymmetry has also been previously found in high-speed images from a patient with functional dysphonia where biphonation (coexistence of two fundamental frequencies) was observed [18]. In our experiment, spatiotemporal chaos, a much more complex spatiotemporal pattern than biphonation, was observed. When subglottal pressure was as high as 36 cm H_2O, the spatial correlation $C_{\max}$ of two sides of glottal movement was sufficiently decreased from the reference

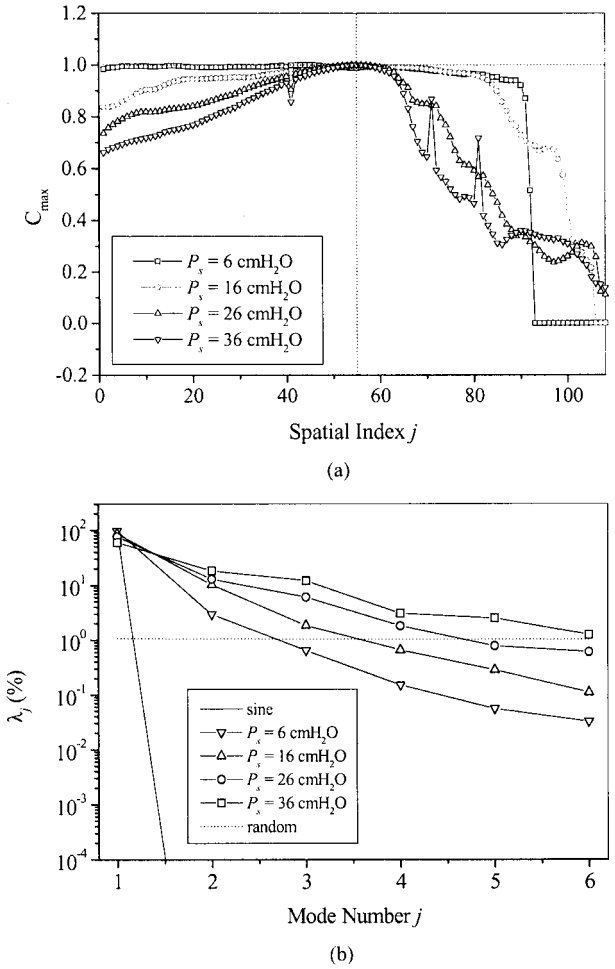

FIG. 3. (a) Spatial correlation function $C_{\max}(i)$ vs spatial index i, where the spatial index of the reference point is $j=54$. (b) The estimated eigenvalue spectrum λ_j versus the model number j, where the curves correspond to the random spatiotemporal series, 36 cm H_2O, 26 cm H_2O, 16 cm H_2O, 6 cm H_2O, and the sine series with uniform spatial distribution.

point ($j=54$), and thus the correlation length L was decreased to 25%. High subglottal pressure breaks down the spatial coherence of the vocal fold vibrations, which may induce spatiotemporal chaos.

In order to further quantify the spatiotemporal complexity of the vocal fold vibrations, we apply eigenmode analysis via Karhunen-Loeve decomposition (KLD), which has proven to be a powerful tool in describing spatiotemporal chaos [4,6,8,9]. For the vibratory signal $u(j,t)$ extracted with high-speed digital imaging, we can calculate the spatial covariance matrix C_{ij} as [18,19]

$$C_{ij} = \langle \delta u(i,t)\, \delta u(j,t) \rangle_T, \tag{3}$$

where $i,j=1,2,N$ is the spatial index. C_{ij} is a symmetric matrix whose eigenvalue λ_j and eigenvector $\mathbf{Q}_j$ satisfy $\mathbf{C}\mathbf{Q}_j=\lambda_j\mathbf{Q}_j$. The eigenvalue λ_j measures the energy captured by the corresponding eigenvectors $\mathbf{Q}_j$. The relative energy E_k of the kth eigenmode can be described as $E_k=\lambda_k/\Sigma_{j=1}^N\lambda_j$. The eigenvectors or eigenmodes $\mathbf{Q}_j$ form a complete orthonormal set $\Sigma_{k=1}^N\mathbf{Q}_i(k)\mathbf{Q}_j(k)=\delta_{ij}$, and then the vibratory signal $u(j,t)$ can be expanded as

$$u(k,t) = \langle u(k,t) \rangle_T + \sum_{j=1}^{N} a_j(t) Q_j(k), \tag{4}$$

where the temporal modal coefficients are $a_j(t)=\Sigma_{k=1}^N Q_j(k)\,\delta u(k,t)$. We then calculated the global entropy S from E_k as [8]

$$S = -\lim_{N\to\infty} \frac{1}{\ln N} \sum_{k=1}^{N} E_k \ln E_k. \tag{5}$$

Entropy measures the degree of disorder of a spatiotemporal pattern. Entropy is low for ordered spatiotemporal behavior with the main energy concentrated in the first few modes. For spatiotemporal data with uniform spatial distribution, $S=0$ shows that only one eigenmode with energy $E_1=1$ is needed to describe the dynamics. For a random spatiotemporal pattern, the entropy approaches 1 and the energies are equally spread across all eigenmodes.

Figure 3(b) shows the estimated eigenvalue spectrum of λ_j versus the mode number j, where the curves correspond to a random spatiotemporal series, 36 cm H_2O, 26 cm H_2O, 16 cm H_2O, 6 cm H_2O, and a sine series with uniform spatial distribution. The entropies S of these six spatiotemporal series are given in Table I, where the entropies of the random spatiotemporal series and the sine series are estimated as 1 and 0, respectively. The estimated eigenvalues of the random series approach $1/N$, and the eigenvalues of the sine series are estimated as $\lambda_1\approx 1$ and $\lambda_i\approx 0$ $(i>1)$. For $P_s=6$ cm H_2O, the largest eigenmode has more than 96% energy of the total energy and the entropy is as low as 0.043. However, when P_s was increased to 16, 26, and 36 cm H_2O, their corresponding entropies were increased to 0.107, 0.183, and 0.285, respectively, showing the increased spatiotemporal complexity with P_s. The collapse of spatial coherence characterized by weak spatiotemporal correlation and high global entropy is important evidence of spatiotemporal chaos in vocal fold vibrations driven by high subglottal pressures.

Vocal fold vibration is a highly complex process combining biomechanical and aerodynamic events. Nonlinearity is inherently involved in laryngeal systems through the nonlinear relationship of glottal pressure to airflow, the nonlinear stress-strain properties of tissue, and the nonlinearities of vocal fold collision [12]. High subglottal pressures produce large tissue deformations and strong vocal fold collisions.

TABLE I. Spatial correlation lengths and entropies of spatiotemporal data.

Subglottal pressure (cm H_2O)	Correlation length	Entropy
Sine series	100%	0
P_s=6 cm H_2O	96.8%	0.043
P_s=16 cm H_2O	71.4%	0.107
P_s=26 cm H_2O	33.3%	0.183
P_s=36 cm H_2O	25.0%	0.285
Random series	0	1

Nonlinearities in the mechanical properties of the vocal fold tissue complicate the model structure of the vocal fold system and produce irregular glottal shapes. High velocity airflow passes through the glottis, inducing strong turbulence at glottal constriction and numerous vortices downstream [25]. Fully developed turbulent flow results in random velocity and pressure distributions along the boundary between the airflow and the vocal folds, producing an unsteady aerodynamic force to drive the vocal folds to vibrate. Because of the interactions between turbulent glottal airflow and irregularly shaped vocal folds, it is not surprising that spatiotemporal chaotic patterns are observed in such a complicated vibratory system.

In conclusion, we have presented experimental evidence of spatiotemporal chaos in excised larynx vibrations using high-speed digital imaging. By applying spatiotemporal correlation analysis and the eigenmode analysis via Karhunen-Loeve decomposition (KLD), we investigated the effects of subglottal pressure on the spatiotemporal dynamics of the vocal folds. High subglottal pressure caused spatiotemporal chaotic vocal fold vibrations that were characterized by decreased spatiotemporal correlation length and increased entropy. Physiologically, the mechanical trauma at high subglottal pressure because of overuse and misuse of the vocal folds may result in a variety of human voice disorders, such as vocal nodules and bleeding. Studying human laryngeal disorders at high subglottal pressures is of pathophysiological significance. Canine and human larynges possess physical similarities that allow the canine larynx to be used as an organic model for studying mechanisms of human phonations. Spatiotemporal analysis has been successfully applied to other biomedical systems such as a fibrillating heart [26] and the mammalian visual cortex [9]. This study shows that applying spatiotemporal analysis to high-speed imaging data also has significant importance for understanding the spatiotemporal chaotic mechanisms of disordered voice production and developing new clinical tools for detection of human vocal disorders.

We thank F. A. Feroze for his assistance. This study was supported by NIH Grant Nos. (1-RO1DC006019) and (1-RO1DC05522) from the National Institute of Deafness and other Communication Disorders.

[1] A. Aitta, G. Ahlers, and D. S. Cannell, Phys. Rev. Lett. **54**, 673 (1985).
[2] M. Dubois and P. Berge, J. Fluid Mech. **85**, 641 (1978).
[3] D. J. Patil, B. R. Hunt, E. Kalnay, J. A. Yorke, and E. Ott, Phys. Rev. Lett. **86**, 5878 (2001).
[4] M. Munkel, F. Kaiser, and O. Hess, Phys. Rev. E **56**, 3868 (1997).
[5] Y. Zhang, M. Dai, Y. Hua, W. Ni, and G. Du, Phys. Rev. E **58**, 3022 (1998).
[6] A. Ghosh, V. R. Kumar, and B. D. Kulkarni, Phys. Rev. E **64**, 056222 (2001).
[7] M. C. Cross and P. C. Hohenberg, Rev. Mod. Phys. **65**, 851 (1993).
[8] A. Palacios, G. H. Gunaratne, M. Gorman, and K. A. Robbins, Phys. Rev. E **57**, 5958 (1998).
[9] L. Sirovich, R. Everson, E. Kaplan, B. Knight, E. O'Brien, and D. Orbach, Physica D **96**, 355 (1996).
[10] P. D. Mininni, D. O. Gomez, and G. B. Mindlin, Phys. Rev. Lett. **89**, 061101 (2002).
[11] B. J. Forbes and E. R. Pike, Phys. Rev. Lett. **93**, 054301 (2004).
[12] I. R. Titze, R. Baken, and H. Herzel, "Evidence of chaos in vocal fold vibration," in *Vocal Fold Physiology: New Frontier in Basic Science*, edited by I. R. Titze (Singular, San Diego, 1993), pp. 143–188.
[13] M. S. Fee, B. Shraiman, B. Pesaran, and P. P. Mitra, Nature (London) **395**, 67 (1998).
[14] I. Steinecke and H. Herzel, J. Acoust. Soc. Am. **97**, 1874 (1995).
[15] J. J. Jiang, Y. Zhang, and J. Stern, J. Acoust. Soc. Am. **110**, 2120 (2001).
[16] C. Tao, Y. Zhang, G. Du, and J. J. Jiang, Phys. Rev. E **69**, 036204 (2004).
[17] T. Wittenberg, M. Moser, M. Tigges, and U. Eysholdt, Mach. Vision Appl. **8**, 399 (1995).
[18] J. Neubauer, P. Mergell, U. Eysholdt, and H. Herzel, J. Acoust. Soc. Am. **110**, 3179 (2001).
[19] D. A. Berry, D. W. Montequin, and N. Tayama, J. Acoust. Soc. Am. **110**, 2539 (2001).
[20] J. van den Berg and T. S. Tan, "Results of experiments with human larynxes," Pract. Otorhinolaryngol. (Basel) **21**, 425 (1959).
[21] D. S. Cooper, "Research in laryngeal physiology with excised larynges," in *Otolaryngolgy-Head and Neck Surgery*, edited by C. W. Cummings (Mosby, St. Louis, 1986), Vol. 3, pp. 1766–1776.
[22] J. J. Jiang and I. R. Titze, Laryngoscope **103**, 872 (1993).
[23] J. J. Jiang, Y. Zhang, and C. N. Ford, J. Acoust. Soc. Am. **114**, 1 (2003).
[24] J. Leonardy, F. Kaiser, M. R. Belic, and O. Hess, Phys. Rev. A **53**, 4519 (1996).
[25] A. Barney, C. H. Shadle, and P. O. A. L. Davies, J. Acoust. Soc. Am. **105**, 444 (1999).
[26] F. X. Witkowski, L. J. Leon, P. A. Penkoske, W. R. Giles, M. L. Spano, W. L. Ditto, and A. T. Winfree, Nature (London) **392**, 78 (1998).